ISSN 1674-1056
http://cpb.iphy.ac.cn
http://iopscience.iop.org/cpb
中国物理 B
Chinese Physics
中国物理 Chinese Physics B

## Demonstration of quantum anti-Zeno effect with a single trapped ion

Man-Chao Zhang(张满超), Wei Wu(吴伟), Lin-Ze He(何林泽), Yi Xie(谢艺), Chun-Wang Wu(吴春旺), Quan Li(黎全), Ping-Xing Chen(陈平形)

**Citation:**Chin. Phys. B . 2018, 27(9): 090305. **doi:** 10.1088/1674-1056/27/9/090305

Journal homepage: http://cpb.iphy.ac.cn; http://iopscience.iop.org/cpb

**What follows is a list of articles you may be interested in**

---

## Demonstration of quantum permutation parity determine algorithm in a superconducting qutrit

Kunzhe Dai(戴坤哲), Peng Zhao(赵鹏), Mengmeng Li(李蒙蒙), Xinsheng Tan(谭新生), Haifeng Yu(于海峰), Yang Yu(于扬)
Chin. Phys. B . 2018, 27(6): 060305. **doi:** 10.1088/1674-1056/27/6/060305

## Transitionless driving on local adiabatic quantum search algorithm

Feng-guang Li(李风光), Wan-su Bao(鲍皖苏), Shuo Zhang(张硕), Xiang Wang(汪翔), He-liang Huang(黄合良), Tan Li(李坦), Bo-wen Ma(马博文)
Chin. Phys. B . 2018, 27(1): 010308. **doi:** 10.1088/1674-1056/27/1/010308

## Performance optimization for quantum key distribution in lossy channel using entangled photons

Yu Yang(杨玉), Luping Xu(许录平), Bo Yan(阎博), Hongyang Zhang(张洪阳), Yanghe Shen(申洋赫)
Chin. Phys. B . 2017, 26(11): 110305. **doi:** 10.1088/1674-1056/26/11/110305

## Amplifying and freezing of quantum coherence using weak measurement and quantum measurement reversal

Lian-Wu Yang(杨连武), Yun-Jie Xia(夏云杰)
Chin. Phys. B . 2016, 25(11): 110303. **doi:** 10.1088/1674-1056/25/11/110303

## Promote entanglement trapping in photonic band gaps

Han Wei, Zhang Ying-Jie, Yan Wei-Bin, Xia Yun-Jie
Chin. Phys. B . 2014, 23(11): 110304. **doi:** 10.1088/1674-1056/23/11/110304

---

# Demonstration of quantum anti-Zeno effect with a single trapped ion*

Man-Chao Zhang(张满超)[1,2,†], Wei Wu(吴伟)[1,2,†], Lin-Ze He(何林泽)[1,2], Yi Xie(谢艺)[1,2], Chun-Wang Wu(吴春旺)[1,2,‡], Quan Li(黎全)[1,2], and Ping-Xing Chen(陈平形)[1,2,§]

[1] *Department of Physics, College of Liberal Arts and Sciences, National University of Defense Technology, Changsha* 410073, *China*
[2] *State Key Laboratory of High Performance Computing, National University of Defense Technology, Changsha* 410073, *China*

(Received 22 May 2018; revised manuscript received 19 June 2018; published online 28 August 2018)

We experimentally demonstrate the quantum anti-Zeno effect in a two-level system based on a single trapped ion $^{40}Ca^{+}$. In the large detuning regime, we show that the transfer from the ground state to the excited state can be remarkably enhanced by the inserted projection measurements. The inserted measurements in our experiment are realized by the electron shelving technique. Compared to the ideal projection measurement, which makes the quantum state collapse instantaneously, a practical electron shelving process needs a finite time duration. The minimum time for this collapse process is shown to be inversely proportional to the square of the coupling strength between the measurement laser and the system.

**Keywords:** quantum anti-Zeno effect, single trapped ion, quantum measurement

**PACS:** 03.67.Ac, 32.80.Qk, 42.50.Ct **DOI:** 10.1088/1674-1056/27/9/090305

## 1. Introduction

The quantum Zeno effect (QZE), which is named after the Greek philosopher Zeno who proposed the well-known arrows paradox,[1] predicts that coherent evolution from any initial quantum state can be slowed down by measuring the system frequently enough.[2–7] On the contrary, if the measurements are not frequent enough, the temporal evolution can sometimes be enhanced. This enhancement is known as the quantum anti-Zeno effect (QAZE) or inverse Zeno effect.[8–11] For both the QZE and QAZE, the initial state should be an eigenvector of the measurement operator. QZE and QAZE have attracted widespread interests both theoretically and experimentally due to their relevance to the foundations of quantum mechanics (e.g., quantum measurement[12–14]) as well as possible applications in quantum technologies. To date, they have been investigated in different physical systems, such as the localized atomic system,[15] superconducting current-biased Josephson junction,[16] nanomechanical oscillator,[17] and disordered spin system.[18] In the trapped ion system, the interesting QZE has already been realized by Itano *et al.*,[2] while the equally fascinating QAZE has not been demonstrated yet. Except for the realizations of the QAZE and QZE, the transition from QZE to QAZE,[19–22] as well as the QZE and QAZE subjected to pure dephasing with an initial equal-weight superposition state,[20–22] has also attracted widespread attention.

Theoretically, in the conventional explorations for the QZE as well as QAZE, the von Neumann's projection postulate is assumed. However, as the dynamical QZE, in which no instantaneous projection measurement is involved, is proposed,[11,23,24] and then experimentally realized,[25] some researchers now believe that the projection postulate in the QAZE and QZE is not necessary, and the real measurements that need a duration of time in real-world systems (e.g. the trapped ion system) can also lead to the QZE and QAZE. Thus an interesting question arises, what will happen if the measurement is imperfect?

In this paper, we investigate the QAZE with a single trapped ion $^{40}Ca^{+}$. Firstly, we briefly review the QAZE theory in section 2. Then in section 3, we give the proposal for the QAZE with a trapped ion and introduce the practical collapse measurement, which is realized by the electron shelving technique[26,27] in our experiment. In section 4, we first obtain the minimum time that the inserted collapse measurement process needs by numerically fitting the experimental data. Then, we realize the QAZE by setting the collapse measurement time as 8 μs, and find the oscillating result when the measurement time is less than 8 μs.

## 2. Theoretical model

The theoretical model investigated in this paper resembles that proposed in Ref. [8]. In Alfredo's theory, the system is assumed to have a level structure shown in Fig. 1(a). $|1\rangle$ and $|2\rangle$ are the ground and metastable excited states, respectively. They are coupled by a radiation field with coupling constant

*Project supported by the National Basic Research Program of China (Grant No. 2016YFA0301903), the National Natural Science Foundation of China (Grant Nos. 11174370, 11304387, 61632021, 11305262, 11574398, and N 61205108), and the Research Plan Project of National University of Defense Technology, China (Grant No. ZK16-03-04).

†These authors contributed equally to this paper.
‡Corresponding author. E-mail: cwwu@nudt.edu.cn
§Corresponding author. E-mail: pxchen@nudt.edu.cn

© 2018 Chinese Physical Society and IOP Publishing Ltd 

$\Omega_1$ and detuning $\delta_1$. The Hamiltonian of the system in interaction picture has the form ($\hbar = 1$)

$$H_{\rm I} = -\delta_1|2\rangle\langle 2| + \frac{\Omega_1}{2}(|1\rangle\langle 2| + |2\rangle\langle 1|). \tag{1}$$

If the system is in state $|1\rangle$ initially, the probability of the system in state $|2\rangle$ at $t_1$ is

$$P_2(t_1) = \frac{1}{m^2+1}\sin^2(\Omega_1' t_1/2), \tag{2}$$

where $\Omega_1' = \sqrt{\Omega_1^2 + \delta_1^2}$ and $m = \delta_1/\Omega_1$. This is simply the Rabi oscillation of the system, as shown in Fig. 1(b) with the sine-type curves. It can be concluded that when $|m|$ is large enough, the system always stays in the state $|1\rangle$.

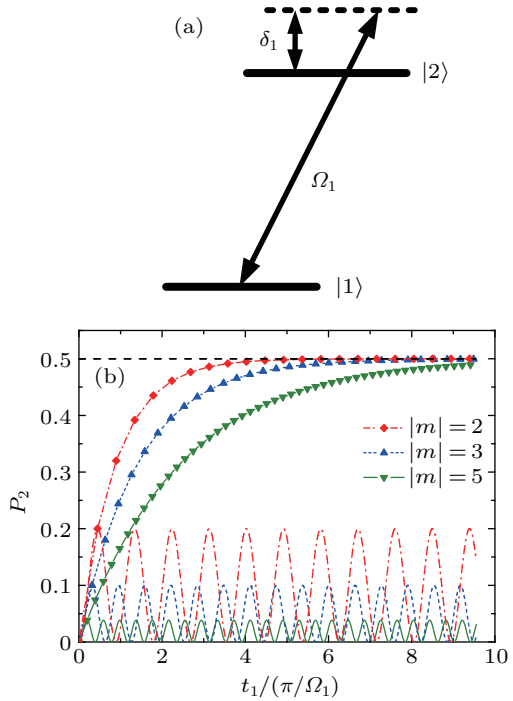



**Fig. 1.** (color online) (a) Scheme of a two-level system driven by a radiation field. (b) Graphs of the theoretical QAZE. The sine-type curves show the evolution of probability $P_2$ in the non-measurement case with varied $|m| = 2, 3, 5$, while the lines with special marks denote $P_2$ when there are measurements, respectively. Note that the measurements can enhance the transition $|1\rangle \to |2\rangle$ to an upper bound of 0.5 (black dashed line).

If $n$ projection measurements performed in the basis $\{|1\rangle, |2\rangle\}$ are inserted at time $kt_1/n$, $(k = 1, \ldots, n)$, and the measurements are assumed to be instantaneous and ideal, these measurements will cause collapses of the wavefunction to the initial state $|1\rangle$. The occupation probability of the state $|2\rangle$ can be written as[8]

$$P_2(n\tau) = \frac{1}{2} - \frac{1}{2}\left[1 - \frac{2}{m^2+1}\sin^2(\Omega_1'\tau/2)\right]^n, \tag{3}$$

where $\tau = t_1/n$ is the interval between two adjacent projection measurements. And the measurement interval that separates the QZE regime and QAZE regime is $\tau_0 = \frac{2}{n\Omega_1^2}\ln(1 + \frac{1}{m^2})$. For the QZE, $\tau < \tau_0$, while for the QAZE, $\tau > \tau_0$. Note that the survival probability (SP) $P_1(t) = 1 - P_2(t)$ that the system is still in its initial state $|1\rangle$ does not meet the assumption $P_1(n\tau) = [P_1(\tau)]^n$ in most studies,[20,21] the result of each measurement should be considered in our research.

Under the condition $|m| > 1$, equation (3) indicates that the probability of state $|2\rangle$ increases monotonically toward 0.5 as $n$ goes to infinity with a certain $\tau$, while in the case of no measurements, $P_2$ is less than 0.5. The lines with special marks in Fig. 1(b) show the results of Eq. (3), and we have set $\tau = t_\pi = \pi/\Omega_1'$ for simplicity. Comparing the results of repeated measurements (lines with marks) and no measurements (sine-type curves), we find that when the measurements exist, the transition $|1\rangle \to |2\rangle$ can be enhanced. This is the so-called QAZE, and the conditions are $|m| > 1$ as well as $\tau > \tau_0$.

## 3. Experimental proposal

In this section, a proposal for realizing the model in section 2 with a single trapped $^{40}Ca^+$ ion is discussed. Figure 2(a) shows the relevant levels and transitions of a trapped ion $^{40}Ca^+$. The coherent-evolution-related states $|1\rangle$ and $|2\rangle$ in Fig. 1(a) are defined by the Zeeman sublevels $4^2S_{1/2}(m_j = -1/2)$ and $3^2D_{5/2}(m_j = -5/2)$, respectively. They are coupled by the electric quadrupole transition $4^2S_{1/2} \leftrightarrow 3^2D_{5/2}$ at 729 nm. $3^2D_{5/2}(m_j = -5/2)$ is a component of the metastable D-orbital that has a long lifetime 1.17 s, so that its spontaneous emission is negligible. $4^2P_{1/2}(m_j = \pm 1/2)$ are two short-lived Zeeman levels with lifetime 7.1 ns. They are ideal levels that we can make use of to realize the measurement, i.e., the electron shelving technique[26,27] in trapped ion system, by coupling to $4^2S_{1/2}(m_j = \pm 1/2)$ levels with a linearly polarized 397-nm laser.

Next we introduce the complete control sequence in our experiment. As shown in Fig. 2(b), the state initialization step is applied first. After that, the trapped ion is prepared in state $|1\rangle$. Next is the repeated $n$ cycles of coherent evolution and collapse measurement. In the coherent evolution stages, the 729-nm beam that couples the states $|1\rangle$ and $|2\rangle$ turns on for time $\tau$, during which the evolution that the system undergoes is governed by equation (1). The repeated collapse measurements realized by the electron shelving technique are applied for time $t_2$ to project the ion state to $|1\rangle$ or $|2\rangle$. Note that the ion may stay in level $4^2S_{1/2}(m_j = 1/2)$ after a collapse measurement, an additional optical pumping process by left-circularly polarized 397-nm laser is needed to drive the ion back to state $|1\rangle$. Finally, a state detection process is applied to distinguish the final state of the system. Here, both the collapse measurement inserted in the coherent manipulation and the final state detection processes are realized by a linearly polarized 397 nm laser. The difference is that the final state detection lasts much longer than the collapse measurements.

The main reason is that in the collapse measurement stages, we only need to prompt the state collapse, or in other words, to reset all the nondiagonal elements of the density matrix to zero, while in the state detection stage, more time is required to collect enough flourescence photons for an efficient state readout.

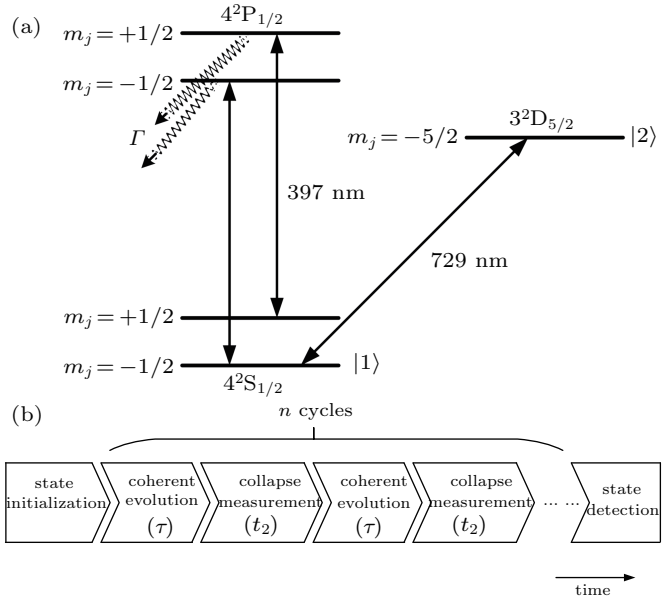



**Fig. 2.** (a) Diagram of the Zeeman sublevels used in coherent evolution and measurement. The $m_j$ represents the magnetic quantum number that corresponds to the Zeeman sublevel. The states labeled $|1\rangle$ and $|2\rangle$ correspond to those in Fig. 1, and the spontaneous decay from $|2\rangle$ to $|1\rangle$ is negligible. (b) Control sequence in our experiment.

## 4. Experimental results

In our experiment, the $^{40}Ca^+$ ion is trapped in a blade Paul trap[28] which is operated at 13.3 MHz and the secular frequencies are 1.6 MHz and 1.0 MHz for radial and axial directions, respectively. In order to drive the $|1\rangle \leftrightarrow |2\rangle$ quadrupole transition, we use a semiconductor laser at 729 nm. This laser source is locked to a high fineness ultra-stable cavity by the Pound–Drever–Hall (PDH) method, and the linewidth is about 20 Hz. The repeated collapse measurement is achieved by applying stabilized semiconductor lasers at 397 nm. It is locked to the transfer cavity which is referred to the ultra-stable 729-nm laser. Laser beams used in the experiment are switched by the acousto-optic modulator (AOM), which has a rise or fall time of about 25 ns and on-to-off ratio of about 35 dB. Lasers at 729 nm and 397 nm are controlled by the cascade of two AOMs in order to avoid a light leak. For the final state detection, a photomultiplier tube (PMT) is used to collect the 397-nm spontaneous radiation emitted from the ion.

Our experiment is based on the control sequence shown in Fig. 2(b). It starts by trapping an ion in the trap, followed by a state initialization stage including Doppler cooling, optical pumping, and sideband cooling.[29] After this stage, the ion is prepared on state $|1\rangle$ with a probability larger than 97%. The mean number of motional phonons is about 0.05, and the heating rate is 0.005 phonons/ms for the axial mode. Then the coherent evolution, collapse measurement, and final state detection processes are carried out sequentially. In our experiment, the drift of the magnetic field is the main obstacle to obtain a longer coherence time. So the timings of the repeated sequences are synchronized to the phase of the power line in order to avoid line-broadening of the ionic energy states due to magnetic field fluctuations at 50 Hz. We measure the coherence time of this system by scanning the interval between two $\pi/2$ pulses of 729-nm laser, and fitting the excitation state populations with a damped cosine curve, which indicates about 400 μs coherence time. Note that in order to avoid sideband transitions, the detuning of the 729-nm laser is set as $\delta_l < 0$.

To realize the QAZE, we first investigate the minimum $t_2$ (labeled as $t_2^{\rm m}$ below) that a single collapse measurement needs to act as an equivalent ideal projection measurement in our experiment. In the collapse measurement process, the phase terms $u$ and $v$ ($u = \rho_{12} + \rho_{21}$, $v = (\rho_{12} - \rho_{21})/\mathrm{i}$, where $\rho_{12}$ and $\rho_{21}$ are the nondiagonal elements of the density matrix describing the ion state spanned by $|1\rangle$, $|2\rangle$) of the Bloch vector damp with the attenuation rate $|\gamma| = \Gamma\Omega^2/(2\Gamma^2 + 8\delta_l^2 - 16\delta_l\delta + 8\delta^2)$,[30] where $\Omega$ and $\delta$ represent the Rabi frequency and detuning of the 397-nm laser. So we can theoretically calculate the magnitudes of $t_2^{\rm m}$ by $1/|\gamma|$. In particular, $|\gamma|$ is determined by the laser detunings, the decay rate $\Gamma$ of level $4^2P_{1/2}$, and the coupling strength $\Omega$ between the linearly polarized laser at 397 nm and the system. However, in our experiment, $\Omega$ is unknown and also difficult to measure. In fact, we cannot obtain it by extracting the periodicity information of the Rabi oscillation, because the high decay rate $\Gamma$ leads to a rapid damping of the oscillation curve. Here, we give an alternative approach to find $t_2^{\rm m}$ experimentally. The basic idea is that, if the measurement time $t_2$ is greater than $t_2^{\rm m}$, the collapse measurement process can be treated as an ideal projection measurement, thus the excited state probability $P_2$ measured in the final state detection stage of the experimental sequence should be equal or close to the theoretical result $P_2^{\rm th}$ calculated with Eq. (3). Otherwise, if the measurement time $t_2$ is less than $t_2^{\rm m}$, there may be a big difference between the experimental experimental result $P_2$ and the theoretical one. Therefore $t_2^{\rm m}$ can be obtained by comparing the experimental probability $P_2$ with the theoretical prediction $P_2^{\rm th}$. In particular, this approach can also be used to verify the theoretical model in Ref. [30], and to obtain the magnitude of $\Omega$ by fitting the experimental data based on the model. To implement this approach, we repeat the experimental sequence in Fig. 2(b) with various $t_2$, keeping other parameters fixed, and measure the final probability $P_2$, as shown in Fig. 3.

The solid circles in Fig. 3 are the experimental results depicting the probability $P_2$ for various $t_2$ with different pa-

rameter settings as shown in the figure. The parameters in Figs. 3(a)–3(c) are different from each other. Compared to Figs. 3(a)–3(c), the data in Fig. 3(d) are obtained by weakening the power of the linearly polarized laser at 397 nm. Based on the exact numerical analysis of the whole sequence, the experimental data are fitted using our theoretical model as indicated by the solid curves in Figs. 3(a)–3(c) with $\Omega = 3.34(2\pi) \times 10^6$ and in Fig. 3(d) with $\Omega = 2.72(2\pi) \times 10^6$. We find that the theoretical and the experimental results agree within an acceptable error range for all the parameter settings. It is obvious that all the solid curves experience a damped oscillatory tendency when $t_2$ goes up, and the final stable values correspond to the theoretical results $P_2^{\rm th}$ (straight dashed lines) derived from Eq. (3) with the same parameters. Thus $t_2^{\rm m}$ should be assigned the $t_2$ when the oscillation amplitude begins to be small enough. For the case in Figs. 3(a)–3(c), $t_2^{\rm m}$ is around 8 μs, which is smaller than that in Fig. 3(d). Therefore, there may be an inverse proportional relation between $t_2^{\rm m}$ and $\Omega$. In other words, the collapse measurement process may be completed more "instantaneously" if $\Omega$ is big enough.

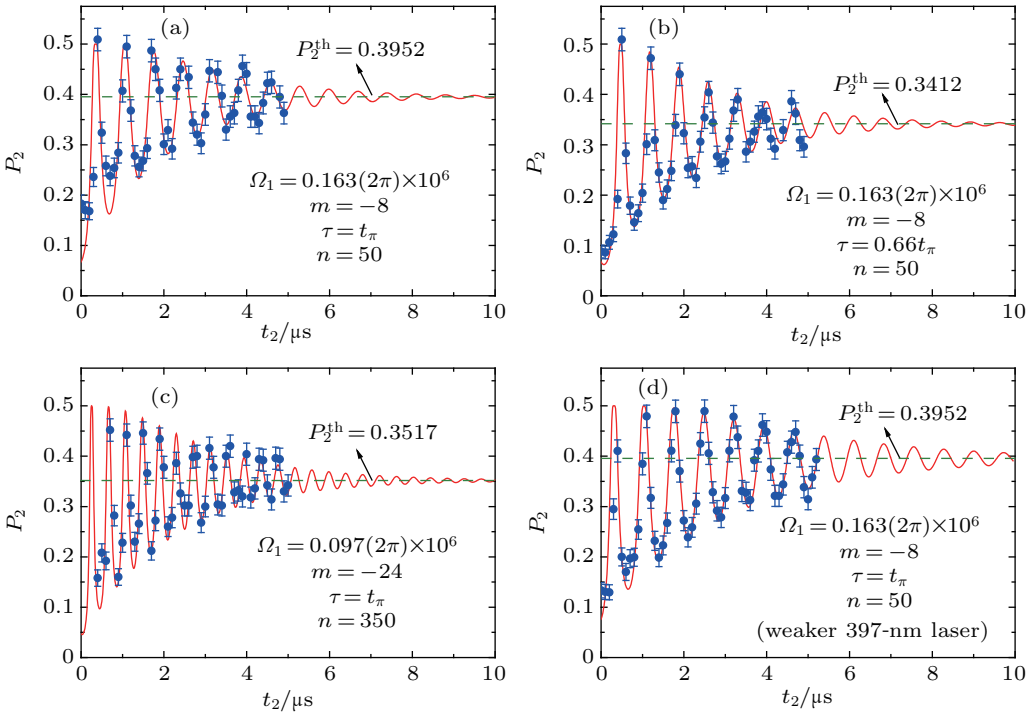



**Fig. 3.** (color online) Probability of finding the ion in state $|2\rangle$ as a function of duration $t_2$ of the collapse measurement process. The experimental data (solid circles) are obtained by repeating the sequence in Fig. 2(b) with the parameters showed in the figures. Compared to (a)–(c), (d) is obtained by weakening the power of the linearly polarized laser at 397 nm. The damped oscillatory curves are the fittings of the experimental data and trend to their stable values when $t_2$ goes up. The straight dashed lines show the theoretical values $P_2^{\rm th}$ with the same parameters by Eq. (2), which correspond to the ideal projection measurement case. Each point represents 500 experiments, and the error bars denote the error of the mean.

For the QAZE achievement, we set the duration of the inserted collapse measurements as $t_2 = 8$ μs. We repeat the experimental sequence in Fig. 2(b) with various $n$ (the number of the inserted collapse measurements), and measure the final probability $P_2$ at the end of each run. The experimental results (solid circles) are shown in Figs. 4(a)–4(c), where the upper bound of the probability, namely, the occupation in state $|2\rangle$, is 0.5. Given the great agreement with the theoretical values (solid curves), it is obvious that the QAZE in our experiment is nearly ideal despite the dephasing by environment. For comparison, we also study the state evolution without inserted collapse measurements. The results (solid squares) are shown in Figs. 4(a)–4(c) and the time duration 8 μs between coherent evolutions is reserved. Note that due to the decoherence of the system, the results here do not reflect the Rabi oscillation as the theoretical results shown in Fig. 1(b) and become larger slowly as the time $t_1$ goes up. By comparing the results above, we find that the probability $P_2$ is larger when the inserted collapse measurements exist. That is to say, the transition $|1\rangle \rightarrow |2\rangle$ increases more rapidly by the inserted collapse measurements. This is exactly the QAZE. And it is obvious that the enhancement can be more remarkable if $|m|$ is smaller. In addition, if we define the transfer rate $\gamma'$ of the transition $|1\rangle \rightarrow |2\rangle$ by $P_2 = 1/2(1-\exp(-\gamma' t_1))$,[20–22] where $t_1 = n\tau$, then the transfer rate $\gamma'$ can be obtained by repeating the sequence in Fig. 2(b) for various measurement intervals $\tau$. The results are shown by the triangles in Fig. 3(d). We find that the experimental results with various $\tau$ also agree with the theoretical values derived from Eq. (3), and the most efficient transfer from $|1\rangle$ to $|2\rangle$ occurs when $\tau = 0.49$ μs$< t_\pi$ under our parameter setting.

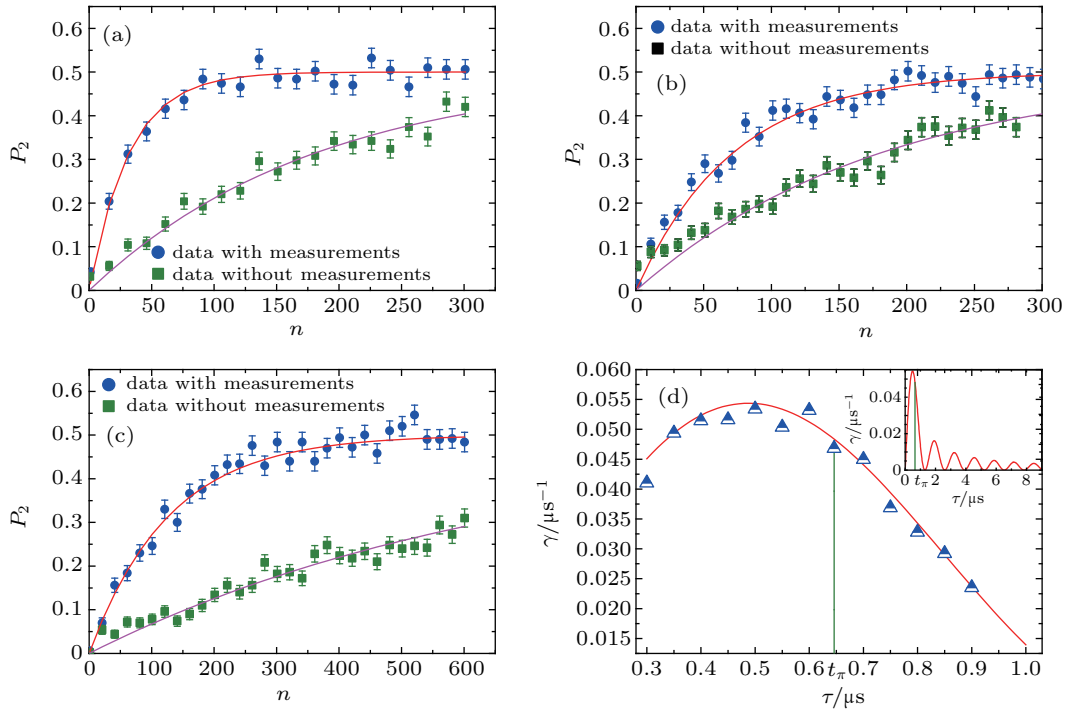



**Fig. 4.** (color online) Anti-Zeno effect with a single trapped $^{40}Ca^{+}$ ion. The duration $t_2$ for electron shelving is set as 8 μs. (a)–(c) The solid circles show the probability $P_2$ of state $|2\rangle$ as a function of the number $n$ of the inserted collapse measurements. They are the experimental results of implementing the sequence in Fig. 2(b) under the conditions of (a) $m = -8$, (b) $m = -12$, and (c) $m = -16$. For simplicity, the measurement intervals here are all set as $\tau = t_\pi$. The solid squares show the state evolution without inserted measurements and the time duration 8 μs between coherent evolutions is reserved. (d) The transfer rate of $|1\rangle \rightarrow |2\rangle$ as a function of the interval $\tau$ between the adjacent measurements. The triangles are the experimental results obtained by repeating the sequence in Fig. 3(a) for various measurement intervals $\tau$ with $\Omega_1 = 0.097(2\pi) \times 10^6$ and $m = -8$. The solid curves represent the theoretical results and the straight solid lines show $\tau = t_\pi$. The inset shows the theoretical transfer rate as a function of interval $\tau$ from 0 to 9 μs, and the straight solid lines also show $\tau = t_\pi$. Each point represents 500 experiments, and the error bars denote the error of the mean.

## 5. Discussion and conclusion

We have realized the QAZE with a single trapped $^{40}Ca^{+}$ ion. The data from our experiment agree well with the theoretical results derived from the theory of QAZE in Ref. [8]. Compared to the non-measurement case, we find that the transfer of population from state $|1\rangle$ to $|2\rangle$ is enhanced by the inserted collapse measurements with an upper bound of 0.5. The inserted collapse measurements in our experiment are realized by the electron shelving technique to cause a complete decoherence of the state. Differing from the ideal projection measurement, which makes the quantum state collapse instantaneously, it needs a finite time duration to drive the phase of the state to zero during the inserted collapse measurement process. And the minimum value of the required measurement time is shown to be inversely proportional to the square of the coupling strength $\Omega$ between the measurement laser and the system. By numerically fitting the experimental data, we obtain the minimum time duration that the inserted collapse measurement needs, and at the same time, estimate the magnitude of $\Omega$.

In addition, by comparing our research with other works, we find that in most studies of the QZE and QAZE, the authors mainly focus on the system coupled only to an environment (bath) during the free evolution stage between measurements. This is actually not the case in our study where a single-mode laser field drives the transition between the ground and excited states. Actually, the QZE and QAZE in our research and other studies have different characteristics. For example, when considering the QAZE in our research, we would rather use the words "enhance the transfer" than "speed up the transition" to describe the effect derived from those measurements because of the excellent promotion of transfer upper bound, and the effect induced from the environment can be ignored. However, in other studies, the QAZE usually refers to the speedup of the induced spontaneous emission or pure dephasing by the environment.

## References

[1] Kofman A G and Kurizki G 2001 *Zeitschrift Für Naturforschung A* **56** 83
[2] Itano W M, Heinzen D J, Bollinger J J and Wineland D J 1990 *Phys. Rev. A* **41** 2295
[3] Petrosky T and Tasaki S and Prigogine I 1990 *Phys. Lett. A* **151** 109
[4] Peres A and Ron A 1990 *Phys. Rev. A* **42** 5720
[5] Block E and Berman P R 1991 *Phys. Rev. A* **44** 1466
[6] Wang X B, You J Q and Nori F 2008 *Phys. Rev. A* **77** 3195
[7] Ren T T, Luo J, Sun X P and Zhan M S 2009 *Chin. Phys. B* **18** 4711
[8] Alfredo L 2003 *Phys. Rev. A* **67** 062113
[9] Kofman A G and Kurizki G 2000 *Nature* **405** 546
[10] Facchi P, Nakazato H and Pascazio S 2001 *Phys. Rev. Lett.* **86** 2699
[11] Ai Q, Xu D, Yi S, Kofman A G, Sun C P and Nori F 2013 *Sci. Rep.* **3** 1752

[12] Huang X S, Xie S Y and Yang Y P 2006 *Acta Phys. Sin.* **55** 2269 (in Chinese)
[13] He Z and Yao C M 2014 *Chin. Phys. B* **23** 110601
[14] Sun S P 2000 *Physics* **29** 457 (in Chinese)
[15] Fischer M C, Gutiérrez-Medina B and Raizen M G 2001 *Phys. Rev. Lett.* **87** 040402
[16] Barone A, Kurizki G and Kofman A G 2004 *Phys. Rev. Lett.* **92** 200403
[17] Chen P W, Tsai D B and Bennett P 2010 *Phys. Rev. B* **81** 115307
[18] Keisuke F and Katsuji Y 2010 *Phys. Rev. A* **82** 5929
[19] Cao X, Ai Q, Sun C P and Franco N 2012 *Phys. Lett. A* **376** 349
[20] Zaman C A and Gong J 2014 *Phys. Rev. A* **90** 165
[21] Wei W and Qing L H 2017 *Phys. Rev. A* **95** 042132
[22] Adam Z C 2016 *Sci. Rep.* **6** 29497
[23] Pascazio S and Namiki M 1994 *Phys. Rev. A* **50** 4582
[24] Layden D, Martinmartinez E and Kempf A 2015 *Phys. Rev. A* **91** 022106
[25] Harrington P M, Monroe J T and Murch K W 2017 *Phys. Rev. Lett.* **118** 240401
[26] Nagourney W, Sandberg J and Dehmelt H 1986 *Phys. Rev. Lett.* **56** 2797
[27] Sasura M and Buzek V 2002 *Optica Acta International Journal of Optics* **49** 1592
[28] Cai L H, Hai W H and Lu G B 2006 *Chin. Phys. B* **15** 2275
[29] Roos C 2000 *Controlling the Quantum State of Trapped Ions* (Ph.D. Dissertation) (University Innsbruck)
[30] Kimble H J, Cook R J and Wells A L 1986 *Phys. Rev. A* **34** 3190